Polyhedron 51 (2013) 222–227

Contents lists available at SciVerse ScienceDirect

Polyhedron

journal homepage: www.elsevier.com/locate/poly

Formation of a Cu(II)–phenoxyl radical complex from a Cu(II)–phenolate complex: A new model for galactose oxidase

Rajib Kumar Debnath [a], Apurba Kalita [b], Pankaj Kumar [b], Biplab Mondal [b,*], Jatindra Nath Ganguli [a,*]

[a] Department of Chemistry, Gauhati University, Guwahati, Assam 781014, India
[b] Department of Chemistry, Indian Institute of Technology Guwahati, Assam 781039, India

ARTICLE INFO

Article history:
Received 4 October 2012
Accepted 21 December 2012
Available online 11 January 2013

Keywords:
2,4-Ditert butyl phenol
Piperazine ethylamine
Manich condensation
Galactose oxidase

ABSTRACT

A new N_3O type tetradentate ligand (HL) [2,4-di-tert-butyl-6-((4-(2-(6,8-di-tert-butyl-2H-benzo[e][1,3]oxazin-3(4H)-yl)ethyl)piperazin-1-yl)methyl)phenol] and its complex $[CuL(CH_3OH)]ClO_4$ (CH_3OH) have been synthesised. The complex has been crystallographically and spectroscopically characterised. It has been noticed that in the presence of acetonitrile the Cu(II) centers in the complex undergo reduction with a concomitant oxidation of the ligand. EPR and UV–Vis spectroscopic studies of the complex in acetonitrile indicate that this disproportionation proceeds via the formation of a Cu(II)–phenoxyl intermediate. The Cu(II)–phenoxyl complex is found to be stable in methanol in the presence of base. The oxidised products of the ligand are isolated and characterized. The paramagnetic centers in the Cu(II)–phenoxyl complexes were found to be weakly ferromagnetically coupled.

1. Introduction

The active sites of the two copper containing enzymes galactose oxidase and glyoxal oxidase are known to contain a coordinated tyrosyl radical [1–6]. Galactose oxidase (GO), the extracellular copper-containing enzyme, is known to catalyse the two-electron oxidation of primary alcohols to the corresponding aldehydes with a simultaneous reduction of dioxygen to hydrogen peroxide [7–13]. An X-ray crystallographic study [14] of the active site of the reduced inactive form of galactose oxidase shows the presence of a mono-nuclear copper(II) center in a square-pyramidal coordination sphere comprised of two tyrosine, two histidine residues and an acetate ion. Previous work shows that this Cu(II) center along with a phenoxyl radical catalyze two electron redox chemistry at the mononuclear active site [9,15]. However, the mechanism of the electron transfer processes and structural parameters which play a key role in controlling the stability and reactivity of the coordinated radical in the active form are still not very clear. Here we report the spectroscopic studies of a Cu(II)–phenoxyl radical complex which can mimic the enzymetic active sites. From the single crystal structure of the complex it is seen that the complex is in the phenoxide and not the phenoxyl form. Even in methanol the complex shows the inactive form of the GO model, but in acetonitrile the complex gets activated and conversion takes place from the phenoxide to the phenoxyl form, which is shown by UV–Vis and EPR studies. In acetonitrile the complex also shows catalytic activity for the conversion of some aromatic alcohols to their corresponding aldehydes [16].

2. Results and discussion

The ligand HL has been synthesized using the previously reported methods of a one-pot Mannich synthesis [17–19]. The formation of the ligand has been confirmed by various spectroscopic techniques like FT-IR, ^1H and ^{13}C NMR, elemental analysis and single crystal structure. An X-ray quality single crystal of the ligand was grown by slow diffusion of a dichloromethane solution of the ligand into hexane, followed by slow evaporation. The Ortep diagram for the neutral HL molecule is shown in Fig. 1.

2.1. Structure and spectroscopic properties of the complex

The green complex **1** has been synthesized by the reaction of hexa aqua Cu(II) perchlorate with LH in methanol. The complex was obtained as green microcrystalline precipitates on keeping the reaction mixture at 0 °C for overnight. The formation of the complex has been confirmed by various spectroscopic studies, namely FT-IR, EPR, ESI-Mass, magnetic moment studies, microanalysis and finally by single crystal structure determination. The mono-cationic complex shows satisfactory microanalytical data and behaves as a 1:1 electrolyte in methanol solution.

Fig. 2 represents the ORTEP diagram of complex **1**. The X-ray quality crystals were grown by dissolving the complex in HPLC

* Corresponding authors.
E-mail address: jatin_ganguli_gu@yahoo.co.in (J.N. Ganguli).

0277-5387/$ - see front matter © 2013 Elsevier Ltd. All rights reserved.
http://dx.doi.org/10.1016/j.poly.2012.12.036

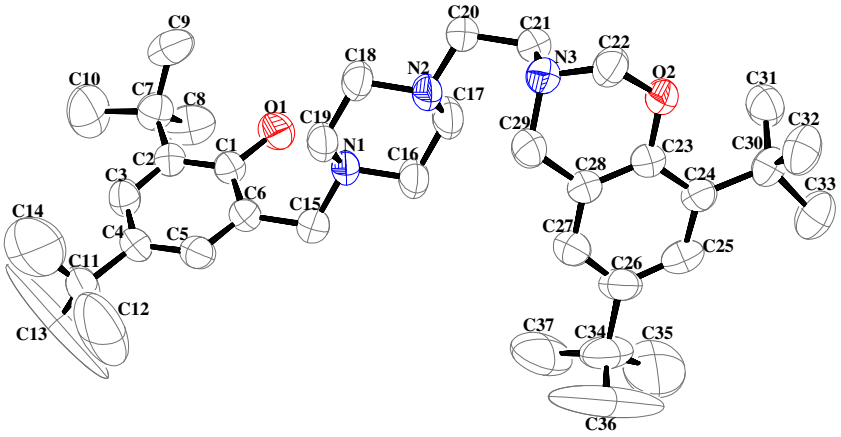

Fig. 1. Ortep plot of LH (50% ellipsoid plot). Hydrogens have been removed for clarity.

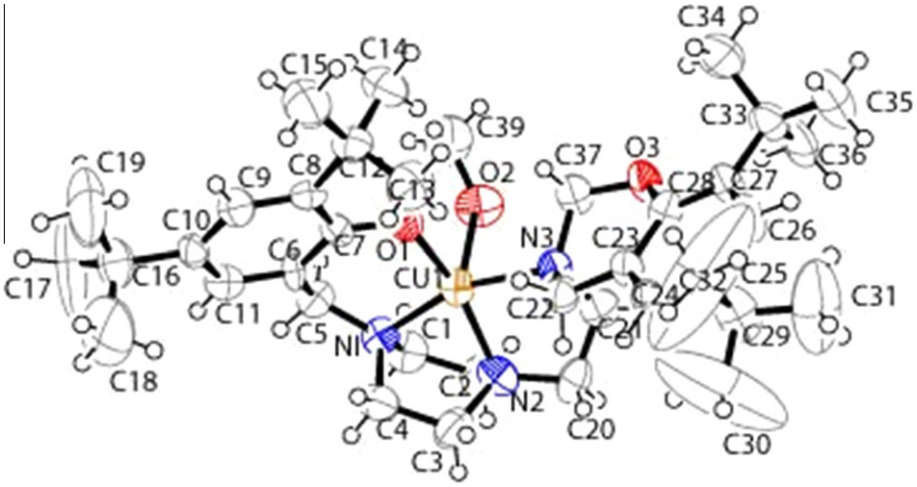

Fig. 2. ORTEP diagram for complex **1** (methanol and perchlorate are removed for clarity).

graded methanol and keeping the solution at 25 °C for three days. The crystal structure reveals that the complex is in a square-pyramidal coordination sphere in which the Cu(II) center is surrounded by three nitrogen and one oxygen atom from the ligand moiety in a square plane, and the fifth coordination site is occupied by a methanol solvent. Here the basal angles are $\beta = 162.93°$ and $\alpha = 159.79°$, thus the trigonality index (τ) value is 0.05 [$\tau = (\beta-\alpha)/60°$] [20], which indicates the complex is present almost in a square pyramidal geometry. The Cu–O_{phen} distance is found to be 1.859(6) Å, which is about 0.1 Å shorter than that of the Cr(III)–O_{phen} distance (1.943 Å) in a Cr(III)–phenoxyl radical complex with the 1,4,7-tris(3-tertbutyl-5-methoxy-2-hydroxybenzyl)1,4,7-triazacyclononane ligand [21]. This because in complex **1** the oxygen of the phenol ring binds Cu in the phenolate form instead of the phenoxyl form. The O1–C7 distance of 1.347 Å is little longer compared to the reported distance in the above said phenoxyl radical complex. It is also on the higher side compared to the calculated distance (1.257 Å) for the free phenoxyl radical, *p*-CH_3–PhO$^{\cdot}$, reported by Hildebrandt et al. [22,23]. The crystallographic data for both complex **1** and the ligand LH are supplied in Table 1. The bond length and bond angle data table for complex **1** are supplied in Table 2 (for the ligand see Supporting information Tables S1 and S2).

The IR spectrum of complex **1** in a KBr disc (Supporting information Figure S9) exhibits a sharp band at 1469 cm^{-1} which can be attributed to the C_1–O stretching vibrations from the phenolate group. The reported values for Cu(II)–coordinated phenoxyl radical complexes were 1497 and 1494 cm^{-1} in complexes $[Cu^{II}(^3L^{met})H]^{+\cdot}$ and $[Cu^{II}(^3L^{met})H_2]^{2+\cdot}$ respectively. [($^3L^{met}$)H_2 = 1,4,7-tris(3-tertbutyl-5-methoxy-2-hydroxybenzyl)1,4,7-triazacyclononane] [25]. In the FT-IR spectra, the presence of the characteristic perchlorate vibrations at ~1100 and 625 cm^{-1} indicates the monocationic complex. The molar conductivity: [$\Lambda_M = 137\ \Omega^{-1}\ cm^2\ mol^{-1}$] indicates that the complex is a 1:1 electrolyte in methanol.

2.2. UV-Vis spectral studies

Fig. 3 shows the electronic spectrum of complex **1** in acetonitrile. The green solution exhibits the $O_{phen} \rightarrow Cu(II)$ and / d–d transition transition in the visible region at 650 nm ($\varepsilon = 1210\ M^{-1}\ cm^{-1}$). The intense absorption at 400 nm ($\varepsilon = 3525\ M^{-1}\ cm^{-1}$) is characteristic for the $\pi \rightarrow \pi^*$ transition of phenoxyl radicals. These are in agreement with the earlier reported phenoxyl complexes [18,25].

The same π–π^* phenoxyl transitions in complexes $[Cu(L)]^{2.2+}$ and $[Cu(LH)]^{2+}$ (H_2L = 1-ethyl-4,7-bis(3-tert-butyl-5-methoxy-2-hydroxybenzyl)-1,4,7-triazacyclononane] are reported to appear at 431, 485 and 431 nm, respectively [24]. It has been found that these phenoxyl radical species are thermally unstable. In addition, they are found to be stable in the presence of base (NaOEt) (Fig. 4) [22].

We have found that the complex is stable in methanol, but in acetonitrile solvent it readily turns colourless in air at room tem-

Table 1
Crystallographic data for the complex $[CuL(CH_3OH)]ClO_4{\cdot}CH_3OH$ and LH.

	$[CuL(CH_3OH)]ClO_4{\cdot}CH_3OH$	LH
Formula	$C_{39}H_{65}ClCuN_3O_8$	$C_{37}H_{59}N_3O_2$
Molecular weight	802.93	577.87
Crystal system	monoclinic	monoclinic
Space group	*P*21/*c*	*P*21/*c*
T (K)	296(2)	296(2)
λ (Å)	0.71073	0.71073
a (Å)	11.598(2)	5.9429(6)
b (Å)	10.1758(18)	39.758(3)
c (Å)	37.589(6)	15.7862(16)
α (°)	90.00	90.00
β (°)	100.094(11)	101.015(6)
γ (°)	90.00	90.00
V (Å^3)	4367.5(13)	3661.2(6)
Z	4	4
D_{calc} (Mg m^{-3})	1.221	1.048
Absorption coefficient (mm^{-1})	0.610	0.064
F(000)	1720	1272.0
Total no. of reflections	10867	9029
Reflections, $I > 2\sigma(I)$	5054	8456
Max. 2θ (°)	28.28	28.44
Ranges (*h*, *k*, *l*)	$-10 \leqslant h \leqslant 10$, $-8 \leqslant k \leqslant 9$, $-34 \leqslant l \leqslant 34$	$-7 = h \leqslant 7$, $-53\ k \leqslant 53$ $-20\ l \leqslant 20$
Complete to 2θ (%)	99.00	98.20
Refinement method	full-matrix least-squares on F^2	full-matrix least-squares on F^2
Data/restraints/ parameters	8249/0/360	0.2101
wR_2(all data)	0.1776	0.956
Goodness-of-fit (GOF) on (F^2)	1.112	0.0737
R indices [$I > 2\sigma(I)$]	0.0798	0.2123
R indices (all data)	0.0983	

perature and yields the colorless crystals of $[Cu(CH_3CN)_4]ClO_4$ and the modified ligands L′ (6,8-di-tert-butyl-3,4-dihydro-3-(2-(piperazin-1-yl)ethyl)-2H-benzo[e][1,3]oxazine) and 3,5-di-tert-butyl-2-hydroxy-benzaldehyde. This reaction has also been found to take place under dinitrogen. Similar results have been reported by Yamauchi and coworkers [18,26]. It should be noted that these reductions are found to be associated with the concomitant decomposition of the ligand HL to L′ along with 3,5-di-tert-butyl-2-hydroxybenzaldehyde (Scheme 1) (Supporting information, Figs. S16–20).

Table 2
Selected bond lengths (Å) and bond angles (°) of complex **1**.

Bond length (Å)	Complex **1**	Bond angle (°)	Complex **1**
Cu(1)–N(1)	1.971(7)	N(1)–Cu(1)–N(2)	75.0(3)
Cu(1)–N(2)	2.006(8)	N(1)–Cu(1)–N(3)	159.8(3)
Cu(1)–N(3)	2.052(7)	N(1)–Cu(1)–O(1)	98.1(3)
Cu(1)–O(1)	1.859(6)	N(1)–Cu(1)–O(2)	96.6(3)
Cu(1)–O(2)	2.470(7)	N(2)–Cu(1)–N(3)	84.9(3)
N(1)–C(1)	1.490(11)	N(2)–Cu(1)–O(1)	162.9(3)
N(1)–C(4)	1.485(11)	N(2)–Cu(1)–O(2)	103.7(3)
N(1)–C(5)	1.460(10)	N(3)–Cu(1)–O(1)	100.6(3)
N(2)–C(2)	1.460(12)	N(3)–Cu(1)–O(2)	90.0(3)
N(2)–C(3)	1.482(12)	C(1)–N(1)–Cu(1)	104.8(6)
N(2)–C(20)	1.502(11)	C(1)–N(1)–C(4)	106.2(7)
N(3)–C(21)	1.484(11)	C(1)–N(1)–C(5)	113.0(7)
N(3)–C(22)	1.474(11)	C(4)–N(1)–Cu(1)	102.3(5)
N(3)–C(37)	1.453(10)	C(4)–N(1)–C(5)	114.4(7)
O(1)–C(7)	1.347(10)	C(5)–N(1)–Cu(1)	115.0(5)
O(2)–C(39)	1.424(12)	C(2)–N(2)–Cu(1)	104.0(6)
O(3)–C(28)	1.393(10)	C(2)–N(2)–C(3)	107.4(8)
O(3)–C(37)	1.415(10)	C(2)–N(2)–C(20)	113.3(8)
Cl(1)–O(4)	1.391(12)	C(3)–N(2)–Cu(1)	102.2(6)
Cl(1)–O(5)	1.365(10)	C(3)–N(2)–C(20)	116.7(8)
Cl(1)–O(6)	1.379(9)	C(20)–N(2)–Cu(1)	111.9(6)
Cl(1)–O(7)	1.383(10)	Cu(1)–N(3)–C(21)	103.3(5)
O(8)–C(38)	1.343(15)	Cu(1)–N(3)–C(22)	110.2(5)
		Cu(1)–N(3)–C(37)	114.4(5)
		C(21)–N(3)–C(22)	111.1(7)
		C(21)–N(3)–C(37)	110.4(7)
		C(22)–N(3)–C(37)	107.5(7)

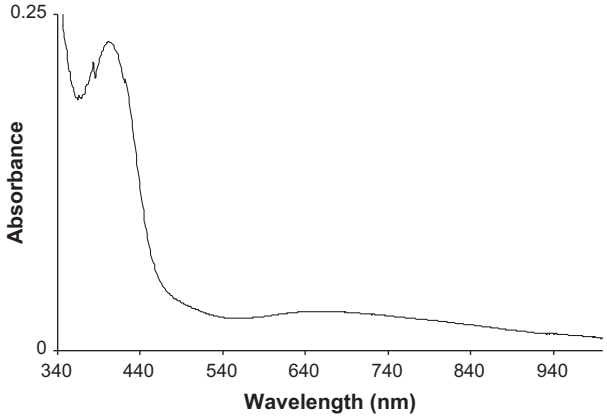

Fig. 3. UV–Vis spectrum of complex **1** in acetonitrile.

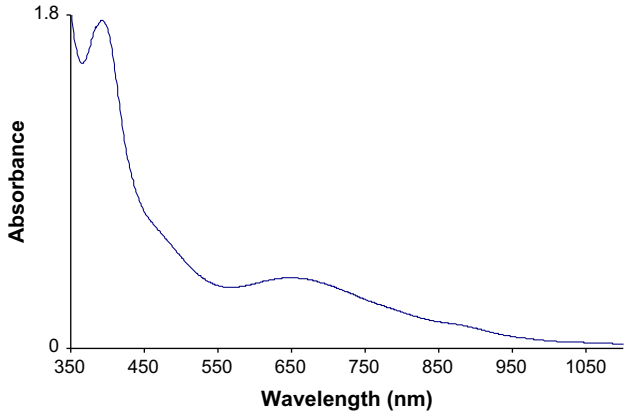

Fig. 4. The UV–Vis spectrum of the Cu(II)–phenoxyl radical complex generated from complex **1** in methanol in the presence of NaOEt.

2.3. EPR studies

The X-band EPR spectrum of complex **1** has been recorded in methanol solution at room temperature and the complex displays the expected characteristic axial spectrum (Supporting information, Fig. S12). Fig. 5 exhibits the X-band EPR spectrum of complex **1** in acetonitrile solvent at room temperature. It is interesting to note that in acetonitrile solvent the complex displays four distinct lines, signals characteristic for a square-pyramidal Cu(II) center having a $d_{x^2-y^2}$ ground state along with a sharp isotropic radical signal in the X-band EPR spectrum at room temperature which is characteristic of a spin triplet state with very weak ferromagnetic coupling. The Cu(II) signals appear at $g_{ave} = 2.11$ and the sharp isotropic signal is for the organic radical ($g = 1.998$) (phenoxyl) (Fig. 5) [27–29]. The broad four line signal for Cu(II) and the radical signal have been found to disappear with time and in equal proportions, indicating an immediate reaction between the Cu(II) center and the phenoxyl radical (Fig. 6). This further supports the formation of only one phenoxyl radical, though there are two phenolate groups. Shimazaki et al. have reported that N_2O_2 type tripodal ligands with stoichiometric amounts of Cu(II) perchlorate results in a Cu(II) phenoxyl radical and Cu(I) in a disproportionation reaction [18,26]. On

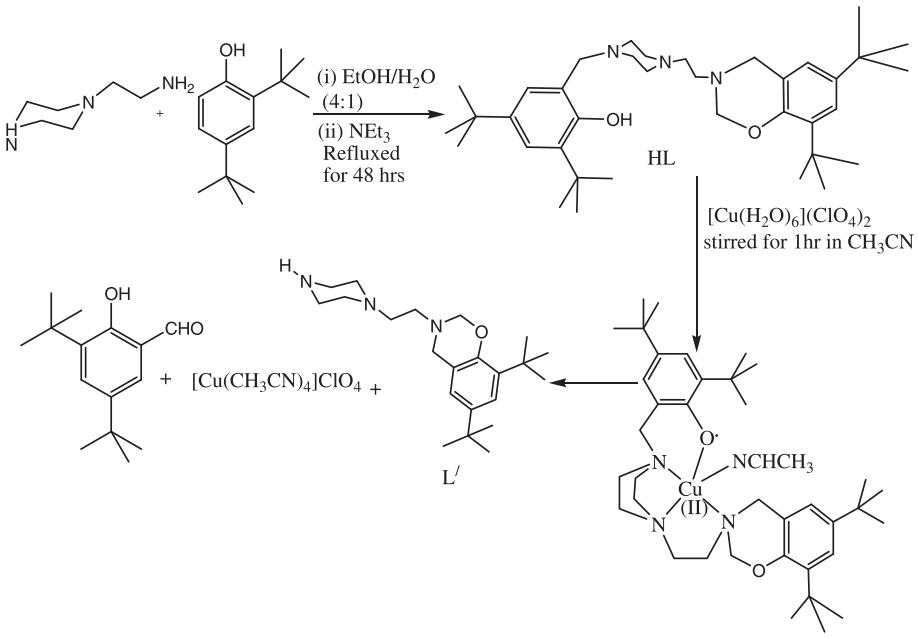

Scheme 1.

Synthetic procedures

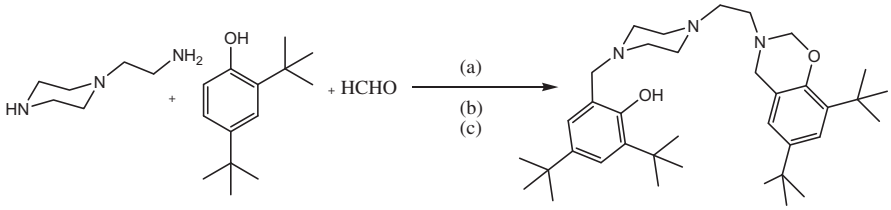

(a) Ethanol and water in 4:1 ratio

(b) NEt_3 as catalyst

(c) Refluxed for 48 hr at 50 °C

Scheme 2.

the other hand, Stack et al have reported Cu(III) complexes by disproportionation of Cu(II) [30]. Our present observations clearly indicate the disproportionation through Cu(II)–phenoxyl radical complex formation. The sharp signal for the phenoxyl radical has been found to disappear, leaving the characteristic Cu(II) signals, on addition of an equivalent proportion of another organic radical, TEMPO (2,2,6,6-tetramethylpiperidinyloxy, a stable nitroxyl radical) to an acetonitrile solution of complex **1**. In methanolic solution addition of an equivalent proportion of TEMPO shows the presence of a radical signal, indicating the absence of the phenoxyl radical in methanol. This further indicates the co-existence of Cu(II) and the phenoxyl radical in the system. From the single structure of complex **1**, the Cu1–O1–C7 bond angle is 123.7(5)° and the angle between the XY plane and the phenoxyl ring plane is 31.28°; hence according to the Goodenough-Kanamori rules [23] of exchange coupling, the ground state of the phenoxyl copper(II) complex **1** is $1 \geqslant S_t \geqslant 0$.

2.4. Galactose oxidase reactivity

A number of substituted benzyl alcohols have been oxidized into the corresponding aldehydes when stirred with complex **1** in acetonitrile solvent (Table S3). The same reaction does not take place in methanol, even after stirring for 24 h in air at room temperature. However, addition of a few drops of acetonitrile to the

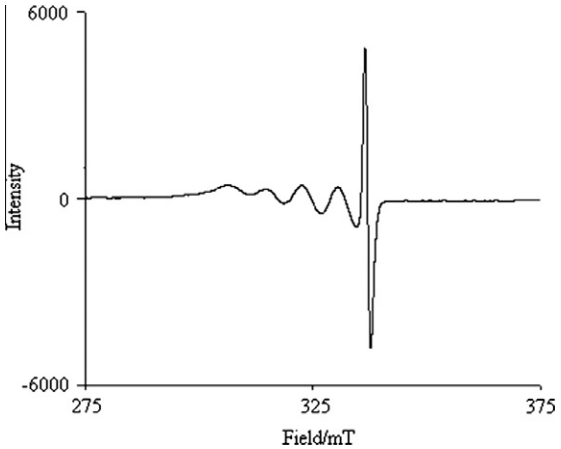

Fig. 5. X-band EPR spectrum of complex **1** in acetonitrile.

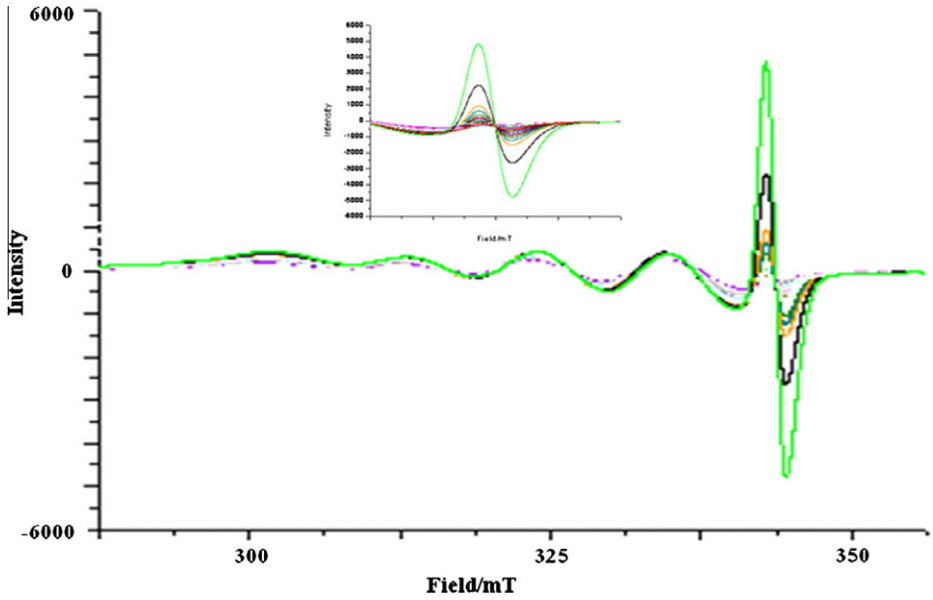

Fig. 6. X-band EPR spectrum of the Cu(II)–phenoxyl radical complex generated from complex **1** in acetonitrile at room temperature. The signals were found to decrease in intensity rapidly with time. Expanded view of the sharp signal in the inset.

methanolic solution leads to the oxidation. This can be attributed to the fact that in the presence of acetonitrile the Cu(II–phenoxyl radical forms, which actively takes part in the oxidation of the primary alcohols.

3. Conclusion

The present study demonstrates a new set of Cu(II) complexes with an N_3O-type ligand as a functional model for the GO active site. It has been found that the Cu(II) centers in the complexes, in the presence of acetonitrile, undergo reduction with a concomitant oxidation of the ligand. The oxidised products of the ligand were isolated and characterized. Spectroscopic studies indicate that this disproportionation proceeds via the formation of a Cu(II)–phenoxyl intermediate. Pyridine also exhibits same reaction as acetonitrile, which indicates the involvement of the exergonic N-donor ligand for the formation of the Cu(II)–phenoxyl complex. The Cu(II)–phenoxyl complex is found to be stable in methanol in the presence of base. The radical complex also catalyzes primary alcohols to the corresponding aldehydes. To the best of our knowledge, the present study demonstrates the first example of the formation of a Cu(II)–phenoxyl complex where the paramagnetic centers are very weakly coupled.

4. Experimental

4.1. General

All reagents and solvents were purchased from commercial sources and were of reagent grade. Acetonitrile was distilled from calcium hydride. Deoxygenation of the solvent and solutions were affected by repeated vacuum/purge cycles or bubbling with nitrogen for 30 min. UV–Vis spectra were recorded on a Perkin Elmer Lambda-25 spectrophotometer. FT-IR spectra were taken on a Perkin Elmer spectrophotometer with the samples prepared as KBr pellets. Solution electrical conductivity was checked using a Systronic 305 conductivity bridge. ^{1}H NMR spectra were obtained with a 400 MHz Varian FT spectrometer. Chemical shifts (ppm) were referenced either with an internal standard (Me_4Si) for organic compounds or to the residual solvent peaks for the copper complexes. The X-Band Electron Paramagnetic Resonance (EPR) spectra of complex **1** and of the reaction mixture were recorded on a JES-FA200 ESR spectrometer, at room temperature as well as at variable temperatures. Elemental analyses were obtained from a Perkin Elmer Series II Analyzer. The magnetic moment of complex **1** was measured on a Cambridge Magnetic Balance.

4.2. Crystal structure analysis

Single crystals were grown by slow diffusion followed by the slow evaporation technique. The intensity data were collected using a Bruker SMART APEX-II CCD diffractometer, equipped with fine focus 1.75 kW sealed tube Mo Kα radiation (λ = 0.71073 Å) at 273(3) K, with increasing ω (width of 0.3° per frame) at a scan speed of 3 s/frame. The SMART software was used for data acquisition. Data integration and reduction were undertaken with SAINT and XPREP software [31]. Multi-scan empirical absorption corrections were applied to the data using the program SADABS [32]. The structures were solved by direct methods using SHELXS-97 and refined with full-matrix least squares on F^2 using SHELXL-97 [33]. All non-hydrogen atoms were refined anisotropically. The hydrogen atoms were located from the difference Fourier maps and refined. Structural illustrations have been drawn with ORTEP-3 for Windows.

4.3. Synthetic procedures

4.3.1. Synthetic procedure for the ligand (LH)

To a solution of 2,4-ditert-butylphenol (4.80 g, 0.023 mol) in EtOH (15 ml) and water (3 ml) was added aqueous formaldehyde (37%, 3.3 g, 0.041 mol), 1-(2-aminoethyl)piperazine (1.29 g, 0.010 mol) and triethylamine (V = 0.500 ml, 0.004 mol) for a catalyst. The resulting solution was kept in an oil bath (at 50 °C) for 48 h (Scheme 2). The white precipitate that formed was filtered, washed with cold MeOH and dried under vacuo over P_2O_5. Yield: 3.845 g (66.52%). The formation of the ligand has been authenticated by its single crystal X-ray structure. An X-ray quality single crystal of the ligand was grown by slow diffusion of a dichloromethane solution of the ligand into hexane followed by slow evaporation. ^{1}H NMR (400 MHz), δ_{ppm}: 1.38 (18H, s), 1.42 (9H, s), 1.44 (9H, s), 2.66 (2H, t), 2.95 (2H, t), 3.73 (2H, s), 4.08 (2H, s), 4.92 (2H, s), 6.80 (1H, s), 6.86 (1H, s), 7.19 (1H, s), 7.23 (1H, s). ^{13}C

NMR (100 MHz), δ_{ppm}: 197.51, 159.25, 149.96, 143.11, 141.77, 137.73, 136.42, 132.02, 128.00, 125.49, 124.93, 122.71, 120.18, 35.17, 34.40, 32.09, 31.82, 31.50, 29.87, 29.47, 29.10, 22.85, 14.30 and elemental *Anal*. Calc. for $C_{37}H_{59}N_3O_2$: C, 77.21; H, 10.06; N, 7.34. Found: C, 77.23; H, 10.07; N, 7.32%. The (m + 1) ion peak at 578.47 in the ESI mass spectrum further supports the formulation (Supporting Information Figures S1, S2, S3 and S4).

*4.3.2. Synthesis of complex **1** in MeOH*

0.370 g (1 mmol) of $[Cu^{II}(H_2O)_6](ClO_4)_2$ was dissolved in 10 ml distilled MeOH. To this solution, 0.577 g (1 mmol) of the ligand L_1 was added slowly with constant stirring. The color of the solution turned green from light blue. Stirring was continued for 1 h at room temperature. The volume of the solution was then reduced to ~2 ml. To this, 10 ml of benzene was added to make a layer on it and the resulting solution was kept overnight in a freezer. This resulted in green coloured crystals of complex **1**. Yield: 0.594 g (80.45%). Elemental *Anal*. Calc. for $C_{39}H_{65}ClCuN_3O_8$: C, 58.34; H, 8.16; N, 5.23; O, 15.94. Found: C, 57.93; H, 8.06; N, 5.43; O, 16.07%. Molar conductivity: [Λ_M = 137 Ω^{-1} cm^2 mol^{-1}].

4.3.3. Isolation of L_1'

185 mg (0.5 mmol) of $[Cu(H_2O)_6](ClO_4)_2$ were dissolved in 15 ml acetonitrile in a round bottom flask. 289 mg (0.5 mmol) of the ligand HL was added to the flask and stirred for an hour. The transient greenish solution became orange over the course of the reaction. The volume of the solution was reduced using a rotavapor and kept in a freezer overnight. $[Cu(CH_3CN)_4](ClO_4)$ was crystallized out. The remaining part was then dried and subjected to column chromatography. The 3,5-di-tert-butyl-2-hydroxybenzaldehyde was separated by hexane. Yield (75%). The amine product, L_1', was eluted with methanol:chloroform (v/v, 1:10) mixture. Yield (70%). 3,5-DI-tert-butyl-2-hydroxybenzaldehyde: ^{1}H NMR (400 MHz, $CDCl_3$), δppm: 1.33 (9H, s), 1.43 (9H, s), 7.35 (1H, s), 7.60 (1H, s), 9.86 (1H, s), 11.66 (1H, s); ^{13}C NMR (100 MHz, $CDCl_3$), δppm: 29.46, 31.52, 34.50, 35.21, 120.18, 128.05, 132.09, 95 137.67, 141.81, 159.29, 197.55. 6,8–Di-tert-butyl-3,4-dihydro-3-(2-(piperazin-1-yl)ethyl)-2H-ebenzo[e][1,3]oxazine, L_1', ^{1}H NMR (400 MHz, $CDCl_3$), δppm: 1.18 (9H, s), 1.27 (9H, s), 2.20 (4H, s), 2.63 (4H, t), 3.58 (4H, s), 3.97 (2H, s), 4.64 (2H, s), 6.69 (1H,s), 7.22 (1H, s); ^{13}CNMR (100 MHz, $CDCl_3$), δppm: 30.01, 31.80, 34.10, 35.06, 45.17, 49.17, 56.01, 64.03 82.89, 122.18, 123.87, 125.26, 136.18, 140.02, 154.12 (Supporting information Figs. S16–S20).

Acknowledgements

The authors would like to thank CSIR, India for providing a scholarship to RKD, DST-FIST, India for the X-ray diffractometer facility, CIF, IIT Guwahati for NMR, Esi-Mass and EPR facilities.

Appendix A. Supplementary material

CCDC 837285 and 95786 contain the supplementary crystallographic data for HL and complex **1** These data can be obtained free of charge via http://www.ccdc.cam.ac.uk/conts/retrieving.html, or from the Cambridge Crystallographic Data Centre, 12 Union Road, Cambridge CB2 1EZ, UK; fax: (+44) 1223 336 033; or e-mail: deposit@ccdc.cam.ac.uk.

References

[1] J.P. Klinman, Chem. Rev. 96 (1996) 2541.
[2] J.W. Whittaker, in: H. Sigel, A. Sigel (Eds.), Metal Ions in Biological Systems, vol. 30, Marcel Dekker, New York, 1994, p. 315.
[3] J.W. Whittaker, Chem. Rev. 103 (2003) 2347.
[4] M.M. Whittaker, P.J. Kersten, N. Nakamura, J. Sanders-Loehr, E.S. Schweizer, J.H. Whittker, J. Biol. Chem. 271 (1996) 681;
M.M. Whittaker, P.J. Kersten, D. Cullen, J.W. Whittaker, J. Biol. Chem. 274 (1999) 36226.
[5] N. Ito, S.E.V. Phillips, C. Stevens, Z.B. Ogel, M.J. Mcpherson, J.M. Keen, K.D.S. Yadav, P.F. Knowles, Nature 350 (1993) 87.
[6] B.A. Jazdzewski, W.B. Tolman, Coord. Chem. Rev. 200 (2000) 633.
[7] D. Amaral, F. Kelly- Falcoz, B.L. Horecker, Methods Enzymol. 9 (1966) 87.
[8] P.S. Tressel, D.J. Kosman, Methods Enzymol. 89 (1982) 163.
[9] R.A. Vander Meer, J.A. Jongejan, J.A. Duine, J. Biol. Chem. 264 (1989) 7792.
[10] J.W. Whittaker, in: M.H. Sigel, A. Sigel (Eds.), Metalloenzymes Involving Amino Acid Residue and Related Radicals, vol. 30, Marcel Dekker, New York, 1994, p. 315.
[11] P.F. Knowles, N. Ito, Perspective in Bio-inorganic Chemistry, vol. 2, Jai Press Ltd., London, 1994.
[12] J.W. Whittaker, in: K.D. Karlin, Z. Tyeklar (Eds.), Bioinorganic Chemistry of Copper, Chapman and Hall Inc., New York, 1993, p. 447.
[13] P. Gamez, I.A. Koval, J. Reedijk, Dalton Trans. (2004) 4079.
[14] M.M. Whittaker, J.W. Whittaker, J. Biol. Chem. 263 (1988) 6074;
M.M. Whittaker, V.L.D. Vito, S.A. Asher, J.W. Whittaker, J. Biol. Chem. 264 (1989) 704;
M.M. Whittaker, J.W. Whittaker, J. Biol. Chem. 265 (1990) 9610.
[15] G.T. Babcock, M.K. El-Deeb, P.O. Sandusky, M.M. Whittaker, J.W. Whittaker, J. Am. Chem. Soc. 114 (1992) 3727.
[16] A. John, M.M. Shaikh, P. Ghosh, Dalton Trans. (2008) 2815.
[17] E.Y. Tshuva, I. Goldberg, M. Kol, Z. Goldscmidt, Organometallics 20 (2001) 3017.
[18] Y. Shimazaki, S. Huth, A. Odani, O. Yamauchi, Angew. Chem. 39 (2000) 1666.
[19] E.Y. Tshuva, I. Goldberg, M. Kol, Z. Goldscmidt, Inorg. Chem. 40 (2001) 4263.
[20] A.W. Addison, T.N. Rao, J. Chem. Soc., Dalton Trans. (1984) 1349.
[21] A. Sokolowski, E. Bothe, E. Bill, T. Weyhermüller, K. Wieghardt, Chem. Commun. (1996) 1671.
[22] J. Müller, A. kikuchi, E. Bill, T. Weyhermüller, P. Hildebrandt, L. Ould-Moussa, K. Wieghardt, Inorg. Chim. Acta. 297 (2000) 265.
[23] J. Müller, T. Weyhermüller, E. Bill, P. Hildebrandt, L. Ould-Moussa, T. Glaser, K. Wieghardt, Angew. Chem. 37 (1998) 616.
[24] H. Sopo, A. Lehtonen, R. Sillanpaa, Polyhedron 47 (2008) 95.
[25] A. Halfen, B.A. Jazdzewski, S. Mahapatra, L.M. Berreau, E.C. Wilkinson, L. Que Jr., W.B. Tolman, J. Am. Chem. Soc. 119 (1997) 8217.
[26] Y. Shimazaki, S. Huth, S. Hirota, O. Yamauchi, Inorg. Chim. Acta 331 (2002) 168.
[27] P. Chaudhuri, K. Wieghardt, in: K.D. Karlin (Ed.), Progress Inorganic Chemistry, vol. 50, John Wiley and Sons Inc., NewYork, 2001, p. 151.
[28] B. Adam, E. Bill, E. Bothe, B. Goerdt, G. Haselhorst, K. Hildenbrand, A. Sokolowski, S. Steenken, T. Weyhermüller, K. Wieghardt, Chem. Eur. J. 3 (1997) 308.
[29] Ademir dos Anjos, A.J. Bortoluzzi, M.S.B. Caro, R.A. Peralta, G.R. Friedermann, A.S. Mangrich, A. Neves, J. Braz. Chem. Soc. 17 (2006) 540.
[30] X. Ribas, D.A. Jackson, B. Donnadieu, J. Mahia, T. Parella, R. Xifra, B. Hedman, K.O. Hodgson, A. Llobet, T.D.P. Stack, Angew. Chem. 114 (2002) 3117.
[31] SMART, SAINT and XPREP, Siemens Analytical X-ray Instruments Inc., Madison, Wisconsin, USA, 1995.
[32] G.M. Sheldrick, SADABS: software for Empirical Absorption Correction, University of Gottingen, Institut fur Anorganische Chemieder Universitat, Tammanstrasse 4, D-3400 Gottingen, Germany, 1999–2003.
[33] G.M. Sheldrick, SHELXS-97, University of Gottingen, Germany, 1997.